Thermoelectric-transport in metal/graphene/metal hetero-structure

2010 Chinese Phys. B 19 037202

(http://iopscience.iop.org/1674-1056/19/3/037202)

Thermoelectric-transport in metal/graphene/metal hetero-structure*

Hu Hao(胡 昊)[a], Cai Jin-Ming(蔡金明)[a], Zhang Chen-Dong(张晨栋)[a], Gao Min(高 敏)[a], Pan Yi(潘 毅)[a], Du Shi-Xuan(杜世萱)[a], Sun Qing-Feng(孙庆丰)[a], Niu Qian(牛 谦)[b], Xie Xin-Cheng(谢心澄)[a,c], and Gao Hong-Jun(高鸿钧)[a]†

[a] *Beijing National Laboratory of Condensed Matter Physics and Institute of Physics, Chinese Academy of Sciences, Beijing* 100190, *China*

[b] *Department of Physics, University of Texas at Austin, USA*

[c] *Department of Physics, Oklahoma State University, Stillwater, Oklahoma* 74078, *USA*

(Received 19 August 2009; revised manuscript received 27 October 2009)

We investigate the thermoelectric-transport properties of metal/graphene/metal hetero-structure. We use a single band tight-binding model to present the two-dimensional electronic band structure of graphene. Using the Landauer–Butticker formula and taking the coupling between graphene and the two electrodes into account, we can calculate the thermoelectric potential and current versus temperature. It is found that in spite of metal electrodes, the carrier type of graphene determines the electron motion direction driven by the difference in temperature between the two electrodes, while for n type graphene, the electrons move along the thermal gradient, and for p type graphene, the electrons move against the thermal gradient.

Keywords: graphene, Landauer–Butticker formula, thermoelectricity, hetero-structure
PACC: 7210, 7215J, 6148

1. Introduction

Two-dimensional carbon-based material, graphene, has received much attention in the last few years for its novel properties, such as the massless Dirac fermion,[1] Berry's phase and abnormal quantum Hall effect.[2] Due to its excellent in-plane transport properties, several potential applications such as electromechanical resonators,[3] p-n junctions[4−6] and transistors[7] were also proposed. Recently, a giant thermoelectric effect[8] and high thermal conductivity[9] were found in graphene systems, thereby making the graphene a potential candidate for thermoelectric power devices. However, most of these investigations are about the in-plane characteristic of single layer graphene; little work has been done on the hetero-structure properties in graphene-based systems either experimentally or theoretically. The successful preparation of epitaxially grown graphene on transition metal surfaces[10−14] makes it possible to study the metal/graphene hetero-structure properties by using scanning tunneling microscopy. Due to its peculiar electronic structure, hetero-structured graphene is expected to have some fantastic phenomena and applications.

In this paper, we build an STM-like model to investigate the thermal transport properties of the metal/graphene/metal system.

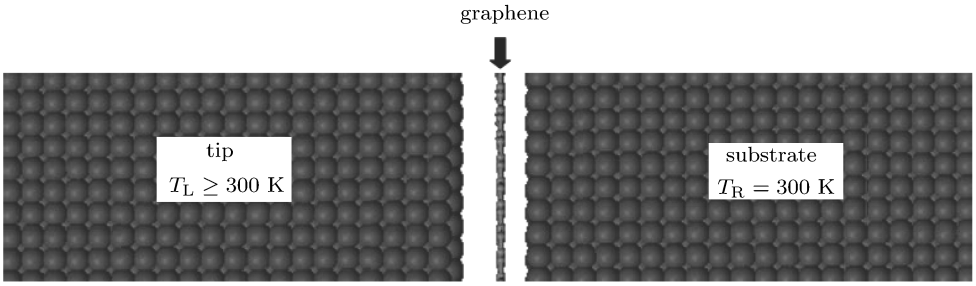

Fig. 1. Schematic diagram of the model of the metal/graphene/metal hetero-structure. The temperature of the right electrode (substrate), $T_{\rm R}$, is constant, and the temperature of the left electrode (tip), $T_{\rm L}$, can vary from 300 to 450 K.

*Project supported by the National Natural Science Foundation of China (Grant No. 60621061), and the National Basic Research Program of China (Grant Nos. 2006CB921305 and 2009CB929103).

†Corresponding author. E-mail: hjgao@aphy.iphy.ac.cn

The model is composed of two metallic electrodes with a single layer of graphite (graphene) in between. In this model, the temperature of the right electrode (substrate) is fixed at room temperature (300 K), while the left electrode (tip) is kept at a higher temperature, which is shown in Fig. 1. For this setup, we treat the electron transport process as a coherent transfer process, while the electron parallel momentum and energy conserve during the process.

2. Method

The Hamiltonian of the model is expressed as

$$\begin{aligned} H = & \sum_{k_\parallel^{\mathrm{L}},k_z} \varepsilon^{\mathrm{L}}_{k_\parallel^{\mathrm{L}},k_z} c^{+}_{k_\parallel^{\mathrm{L}},k_z} c_{k_\parallel^{\mathrm{L}},k_z} + \sum_{k_\parallel^{\mathrm{C}}} \varepsilon^{\mathrm{C}}_{k_\parallel^{\mathrm{C}}} b^{+}_{k_\parallel^{\mathrm{C}}} b_{k_\parallel^{\mathrm{C}}} \\ & + \sum_{k_\parallel^{\mathrm{R}},k_z} \varepsilon^{\mathrm{R}}_{k_\parallel^{\mathrm{R}},k_z} c^{+}_{k_\parallel^{\mathrm{R}},k_z} c_{k_\parallel^{\mathrm{R}},k_z} \\ & + t_1 \sum_{k_z,k_\parallel^{\mathrm{C}},k_\parallel^{\mathrm{L}}} (c^{+}_{k_\parallel^{\mathrm{L}},k_z} b_{k_\parallel^{\mathrm{C}}} + \mathrm{H.c.}) \\ & + t_2 \sum_{k_z,k_\parallel^{\mathrm{C}},k_\parallel^{\mathrm{R}}} (c^{+}_{k_\parallel^{\mathrm{R}},k_z} b_{k_\parallel^{\mathrm{C}}} + \mathrm{H.c.}), \end{aligned} \tag{1}$$

where $\varepsilon^{\mathrm{L}}_{k_\parallel^{\mathrm{L}},k_z}$ and $\varepsilon^{\mathrm{R}}_{k_\parallel^{\mathrm{R}},k_z}$ are the kinetic energies of electrons in the left and right electrodes, respectively; as we use the free electron gas approximation, they satisfy a parabolic dispersion relation. $\varepsilon^{\mathrm{C}}_{k_\parallel^{\mathrm{C}}}$ is the kinetic energy of electrons in the graphene. Because of its two-dimensional characteristic, the momentum has only parallel terms. In a reciprocal lattice, at the K point, the electron is a Dirac fermion,[1,15] and the band structure has two branches. For neutral graphene, the Fermi surface lies at K points, if there is charge transfer between graphene and electrodes, the Fermi surface can be offset from the Dirac point. Positive offset indicates p type graphene, while negative offset indicates n type. Because the coupling between the substrate and the graphene could be either strong or weak (we suppose that the tip and the graphene always have a weak coupling), which corresponds to large or small t_1, we deal with both cases, i.e. the weak coupling case and the strong coupling case. In the weak coupling case, t_1, which indicates the coupling between the left electrode (substrate) and the graphene, is set to be close to t_2, which shows the coupling between the right electrode (tip) and the graphene. For the strong coupling case, t_1 is set to be much larger than t_2.

The transmission coefficient can be expressed as $T = \mathrm{Tr}\{\Gamma_{\mathrm{L}} G^{\mathrm{r}} \Gamma_{\mathrm{R}} G^{\mathrm{a}}\} = \mathrm{Tr}\{\Gamma_{\mathrm{L}} A\}$,[16] where $G^{\mathrm{r,a}}$ is the Green's function, $G_{\mathrm{L,R}}$ is the linewidth function due to coupling to the electrodes, and A is spectral function. For the strong coupling case, the imaginary part of A is the local density of states of graphene, taking the substrate into account. Using the Hamiltonian given in Eq. (1), we can obtain the concrete expression of T to be

$$T = \frac{(2E - 2E_{\mathrm{F}} - 2\delta\varepsilon)^2 \dfrac{4m_{\mathrm{e}}pq}{2\hbar^2\left[E - \dfrac{(\hbar k_\parallel^{\mathrm{L}})^2}{2m_{\mathrm{e}}}\right]}}{(E - E_{\mathrm{F}} - \delta\varepsilon - E^{+})^2 (E - E_{\mathrm{F}} - \delta\varepsilon - E^{-})^2 + (2E - 2E_{\mathrm{F}} - 2\delta\varepsilon)^2 \dfrac{m_{\mathrm{e}}(p+q)^2}{2\hbar^2\left[E - \dfrac{(\hbar k_\parallel^{\mathrm{L}})^2}{2m_{\mathrm{e}}}\right]}}, \tag{2}$$

where $p = L^{\mathrm{L}}|t_1|^2$; $q = L^{\mathrm{R}}|t_2|^2$; L^{L} and L^{R} are the lengths of left and right electrodes in the z direction, respectively; E is the electron energy of the electrode; $k_{||}^{\mathrm{L}}$ is parallel electron momentum in the left electrode; $\delta\varepsilon$ is the offset of the Fermi surface to the Dirac point; E^{-} and E^{+} are the energies of π and π^* bands of graphene, obtained from the tight-binding method, and $E^{+} = -E^{-}$.

For the strong coupling case, the local density of states of graphene ρ is expressed as

$$\rho(k_\parallel, E) = \frac{1}{2\pi} \frac{2[(E - E_{\mathrm{F}} - \delta\varepsilon)^2 + E^{+2}] \cdot \dfrac{2m_{\mathrm{e}}p}{\hbar\sqrt{2m_{\mathrm{e}}E - (\hbar k_\parallel)^2}}}{((E - E_{\mathrm{F}} - \delta\varepsilon)^2 - E^{+2})^2 + (E - E_{\mathrm{F}} - \delta\varepsilon)^2 \dfrac{4m_{\mathrm{e}}^2 p^2}{\hbar^2[2m_{\mathrm{e}}E - (\hbar k_\parallel)^2]}}. \tag{3}$$

To obtain Eq. (3), we use the condition that $p \gg q$. When the temperatures of the two electrodes are different, there appears an electron flow j_{p} in the system, which is given as

$$j_{\rm p} = \frac{1}{h}\int {\rm d}E \left[\frac{L_{\|}^2}{2\pi^2}\int {\rm d}k_{\|,x}^{\rm L}\int {\rm d}k_{\|,y}^{\rm L} T(k_{\|}^{\rm L}, E)\right][f_{\rm L}(E) - f_{\rm R}(E)] = \frac{L_{\|}^2}{2\pi^2 h}\int {\rm d}E\, T_{\rm sub}\,[f_{\rm L}(E) - f_{\rm R}(E)], \quad (4)$$

and a heat current

$$j_{\rm q} = \frac{L_{\|}^2}{2\pi^2 h}\int {\rm d}E\, T_{\rm sub}\,[f_{\rm L}(E) - f_{\rm R}(E)]\,E, \quad (5)$$

where $f_{\rm L}(E)$ and $f_{\rm R}(E)$ are Fermi distribution functions for left and right electrodes, respectively,

$$f_{\rm L}(E) = \{1 + \exp[(E - E_{\rm F})/k_{\rm B}T_{\rm L}]\}^{-1}; \quad (6a)$$

$$f_{\rm R}(E) = \{1 + \exp[(E - E_{\rm F}]/k_{\rm B}T_{\rm R}]\}^{-1}; \quad (6b)$$

$L_{||}$ is the parallel scale of the electrode.

If we add an external bias between the right electrode and the left electrode, and adjust the value to make the electron flow disappear, we can obtain the thermal potential induced by temperature difference. The external bias influences only the Fermi distributions of the two electrodes, and does not change the transmission coefficients. In this case, we can write the Fermi distributions as

$$f_{\rm L}(E) = \{1 + \exp[(E - eV/2 - E_{\rm F})/k_{\rm B}T_{\rm L}]\}^{-1} \quad (7a)$$

and

$$f_{\rm R}(E) = \{1 + \exp[(E + eV/2 - E_{\rm F}]/k_{\rm B}T_{\rm R}]\}^{-1}, \quad (7b)$$

where V is the external bias. Adjusting V such that $j_{\rm p} = 0$, we can obtain the thermoelectric potential $V_{\rm p} = -V$.

3. Results and discussion

Equation (2) describes how transmission coefficient T depends on electron momentum and electron energy. For the weak coupling case, when the first term in the denominator reaches zero, which in k space is a circle around the K point, T could have a unity value, and would decay very fast apart from the circle for the different energy dispersions of electrodes and graphene. The neighbourhood of one K point at (1.7, 0.0) Å^{-1} (1 Å=0.1 nm) is shown in Fig. 2(a). It implies that only electrons with momentum k that is near the K point can contribute to electron transmission in this system, with the Fermi distribution taken into account. For the strong coupling caseas shown in Fig. 2(b), though T would retain a relatively large value at the circle, it is broadened and distorted a lot due to the strong interaction between the left electrode (substrate) and graphene. Then most of electrons contribute to the transmission. Equation (3) describes how the local density of states of graphene, ρ, depends on electron momentum and electron energy. As mentioned above, it is only for the strong coupling case. The local density of states of graphene, ρ, in k space has a similar trend to that of T, but without the effect of the right electrode (tip), thereby leading to a little difference, which is shown in Fig. 2(c).

Figure 3(a) shows that the transmission coefficient, taking on a 'V'-shape curve, varies with energy E for the weak coupling case. It is because of weak coupling that T has only a finite value at the circle shown in Fig. 2(a), i.e. $T(E)$ is roughly proportional to the perimeter of the circle. The 'V' shape is not symmetric due to the electrode influence, and the transmission coefficient T at lower energy is higher than that at higher energy, with respect to the Fermi energy. Positive $\delta\varepsilon$ would shift the 'V'-shape curve towards higher energy, while negative $\delta\varepsilon$ would shift it towards lower energy. Combining the Fermi distribution in Eq. (4) and considering $\delta\varepsilon = 0$ eV for neutral graphene, the lower energy contribution to the transmission is larger than the higher energy contribution, thus the net electron current is from right to left, contrary to the temperature gradient direction. Positive $\delta\varepsilon$, i.e. p type graphene, would enhance this effect; and negative $\delta\varepsilon$, i.e. n type graphene, would reduce the effect, and reverse the electron current direction into being consistent with the temperature gradient, as shown in Fig. 3(b). For the strong coupling case, Fig. 3(c) shows the transmission coefficient $T(E)$ and the local density of states of graphene. The local density of states of graphene has a large peak at $E = E_{\rm F} - \delta\varepsilon$, due to the interaction between the left electrode and the graphene. Although the transmission coefficient is broadened and dispersed in k space as shown in Fig. 2(c), $T(E)$ also takes on a 'V'-shape curve, which would lead to the same behaviour of the thermoelectric properties as that in the weak coupling case, which is shown in Fig. 3(d).

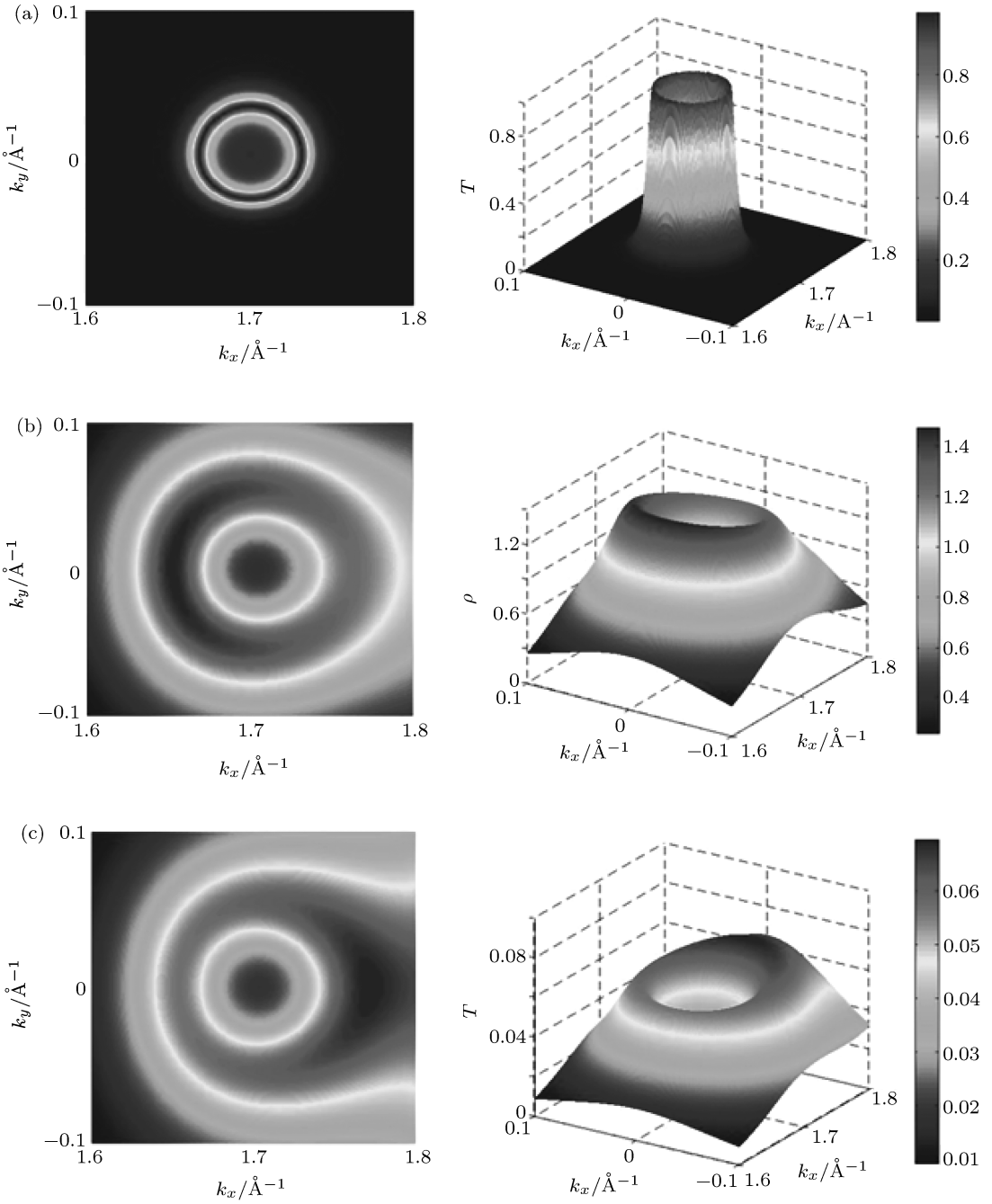

Fig. 2. Transimission function and local density of states in reciprocal space around the Dirac point. The K point is chosen to be at (0.0, 1.70) Å^{-1}, electron energy is set to be 13.2 eV, $\delta\varepsilon$ is 0.0 eV, and the left is the top view. (a) is for the transmission coefficient as a function of momentum (k_x, k_y) of the weak coupling case, where the centre of the circle is the K point. (b) is for the transmission coefficient of the strong coupling case. (c) is for the local density of states of graphene as a function of momentum (k_x, k_y) of the strong coupling case.

The calculated electron current and heat current are shown in Fig. 4. The same as the thermoelectric potential in Figs. 3(b) and 3(d), the electron currents for the weak coupled case and the strong coupled case are along the thermal gradient direction for n type graphene, and against the thermal gradient direction for p type graphene. For the heat current, it is always along the thermal gradient direction, which is consistent with physical intuition and also demonstrates the self-consistency of our model. Note that we do not concentrate on the exact value of the current, but the polarisation, j_{p} and j_{q} are scaled by $10^5 L_{||}^2/2\pi^2 h$ and $10^7 L_{||}^2/2\pi^2 h$ respectively.

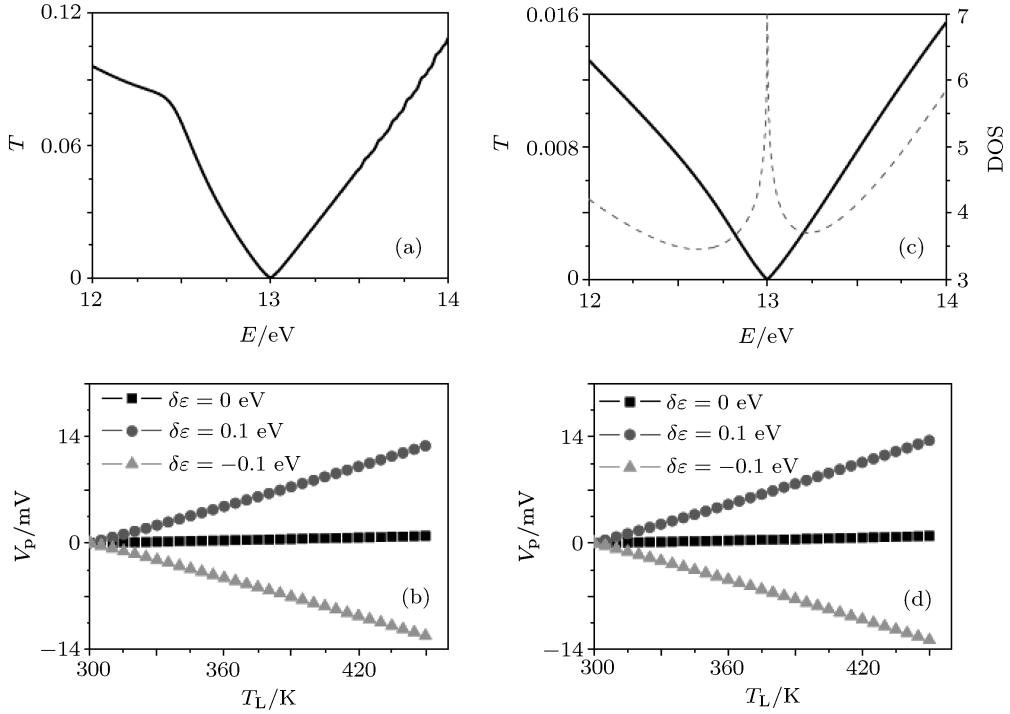

Fig. 3. Simulation results of T and ρ as a function of energy E for the weak coupling case (a) and the strong coupling case (c), simulation results of thermal potential $V_{\rm p}$ as a function of the left electrode temperature $T_{\rm L}$ for the weak coupling case (b) and the strong coupling case (d). For neutron, p type and n type graphene, the values of $\delta\varepsilon$ are set to be 0.0 eV, 0.1 eV and -0.1 eV, respectively.

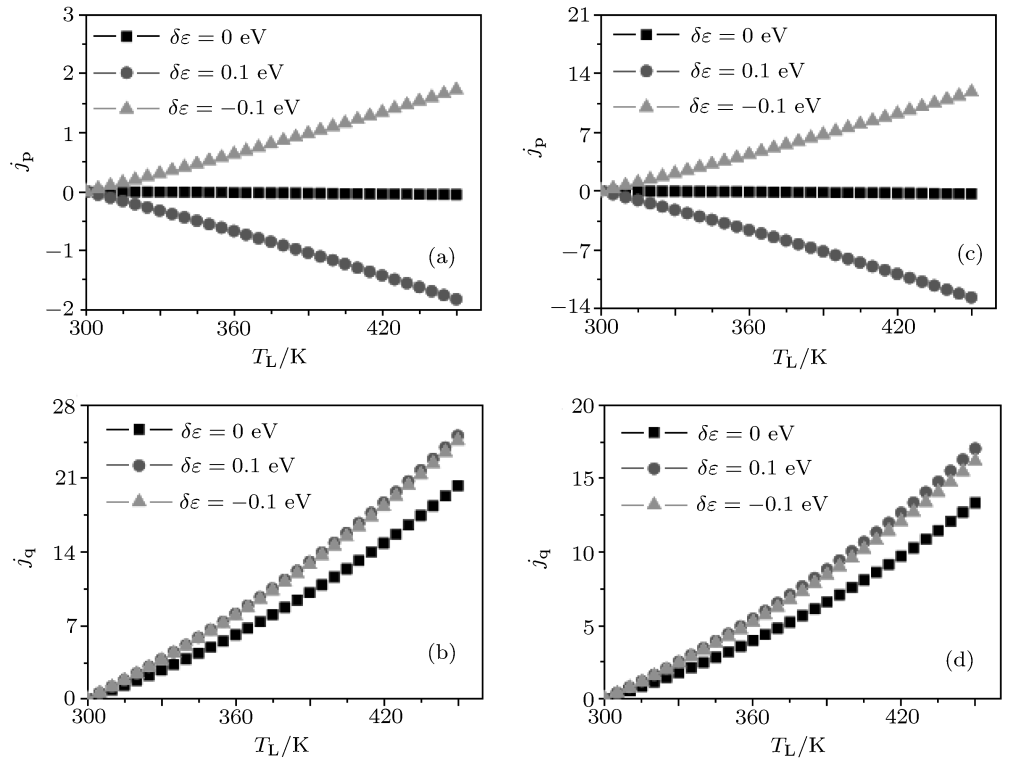

Fig. 4. Calculated electron currents for the weak coupled case (a) and the strong coupled case (c), and heat currents for the weak coupled case (b) and the strong coupled case (d).

Recently, Gao *et al.* investigated the thermoelectric properties for graphene on Pt(111), Ni(111) and Ru(0001) surfaces by using an In-coated STM tip.[15] They found that in a graphene/Pt(111) system, the

electron current driven by the difference in temperature between the substrate and the tip is always against the thermal gradient direction; in a graphene/Ni(111) system, the electron current driven by the temperature difference is always along the thermal gradient direction; in a graphene/Ru(0001) system, the situation is more complicated: the electron current direction is dependent on the tip approaching status.

These phenomena can be explained by our model. For the graphene/Pt(111) system, the graphene interacts weakly with the substrate, and it is of p type,[1)] while for the graphene/Ni(111) system, the graphene interacts strongly with the substrate, and it becomes metallic, then the experimental results are consistent with those obtained from our model. As for the graphene/Ru(0001) system, it is more complicated. The graphene undulates a lot, and the vertical difference between the highest carbon atom and the lowest carbon atom is more than 2 Å.[17,18] Calculation results indicate that the lower part of graphene forms bonds with the Ru substrate and obtains electrons, while the higher part of graphene interacts weakly with the substrate and is a little bit of p type. Then if approaching the tip carefully, when only the higher part of graphene dominates the transport, the electron current would be against the thermal gradient direction; when further approaching the tip, the lower part of graphene dominates the transport, and the electron current would be along the thermal gradient direction.

We emphasise that we use our model here not to simulate the exact value of the thermoelectric properties, but qualitatively give an explanation of the polarisation of the thermoelectric potential, which is determined by the carrier type in the single layer graphene.

We focus on the thermoelectric properties of metal/graphene/metal hetero-structure. In previous work, Ho-Ki Leyo *et al.*[19] used scanning thermoelectric microscopy to probe the local thermoelectric power of semiconductor nanostructures. In their system, the carriers that passed through the junction could be electrons and holes which determined the direction of thermoelectric power. In our system, the carriers in two electrodes are always electrons; the carrier type in the central region determines the direction of thermoelectric power. In Figs. 3(a) and 3(c), we can see that $T(E)$ changes very fast near the Fermi energy, then a large value of Seebeck coefficient is expected,[8] which is consistent with the experiment results.[15]

4. Conclusions

We propose a simple model to investigate the thermoelectric properties of STM-like metal/graphene/metal hetero-structures. It is shown that for p type graphene, the electron current driven by the difference in temperature between the two electrodes is against the thermal gradient direction, while for n type graphene, the electron current is along the thermal gradient direction. Our results are consistent with the recent experimental results.

References

[1] Novoselov K S, Geim A K, Morozov S V, Jiang D, Katsnelson M I, Grigorieva I V, Dubonos S V and Firsov A A 2005 *Nature* **438** 197

[2] Zhang Y B, Tan Y W, Stormer H L and Kim P 2005 *Nature* **438** 201

[3] Bunch J S, van der Zande A M, Verbridge S S, Frank I W, Tanenbaum D M, Parpia J M, Craighead H G and McEuen P L 2007 *Science* **315** 490

[4] Cheianov V V, Fal'ko V and Altshuler B L 2007 *Science* **315** 1252

[5] Williams J R, DiCarlo L and Marcus C M 2007 *Science* **317** 638

[6] Abanin D A and Levitov L S 2007 *Science* **317** 641

[7] Yan Q M, Huang B, Yu J, Zheng F W, Wu J, Gu B L, Liu F and Duan W H 2007 *Nano Lett.* **7** 1469

[8] Dragoman D and Dragoman M 2007 *Appl. Phys. Lett.* **91** 203116

[9] Balandin A A, Ghosh S, Bao W Z, Calizo Irene, Teweldebrhan D, Miao F and Lau C N 2008 *Nano Lett.* 902

[10] Vazquez de Parga A L, Calleja F, Borca B, Passeggi Jr. M C G, Hinarejos J J, Guinea F and Miranda R 2008 *Phys. Rev. Lett.* **100** 056807

[11] Pan Y, Shi D X and Gao H J 2007 *Chin. Phys.* **16** 3151

[12] Pan Y, Zhang H G, Shi D X, Sun J T, Du S X, Liu F and Gao H J 2008 *Adv. Mater.* **20** 1

[13] Coraux J, N'Diaye A T, Busse C and Michely T 2008 *Nano Lett.* **8** 565

[14] Pletikosic I, Kralj M, Pervan P, Brako R, Coraux J, N'Diaye A T, Busse C and Michely T 2009 *Phys. Rev. Lett.* **102** 056808

[15] Katsnelson M I 2007 *Materials Today* **10** 20

[16] Datta S 1995 *Electronic Transport in Mesoscopic Systems* (London: Cambridge University Press) p148

[17] Wang B, Bocquet M L, Marchini S, Gunther S and Wintterlin J 2008 *Phys. Chem. Chem. Phys.* **10** 3530

[18] Sun J T, Du S X, Xiao W D, Hu H, Zhang Y Y, Li G and Gao H J 2009 *Chin. Phys.* B **18** 3008

[19] Lyeo Ho-Ki, Khajetoorians A A, Shi L, Pipe K P, Ram R J, Shakouri A and Shih C K 2004 *Science* **303** 816

[1)] Our first principles calculation demonstrates this, and the results will be published elsewhere.